Received 11 June 2021; accepted 1 July 2021. Date of publication 9 July 2021; date of current version 28 July 2021.

Digital Object Identifier 10.1109/OJCOMS.2021.3096118

Deep Learning Enabled Beam Tracking for Non-Line of Sight Millimeter Wave Communications

RUIYU WANG, PAULO VALENTE KLAINE (Member, IEEE), OLUWAKAYODE ONIRETI (Senior Member, IEEE), YAO SUN (Senior Member, IEEE), MUHAMMAD ALI IMRAN (Senior Member, IEEE), AND LEI ZHANG (Senior Member, IEEE)

School of Engineering, University of Glasgow, Glasgow G12 8QQ, U.K.

CORRESPONDING AUTHOR: L. ZHANG (e-mail: lei.zhang@glasgow.ac.uk)

ABSTRACT To solve the complex beam alignment issue in non-line-of-sight (NLOS) millimeter wave communications, this paper presents a deep neural network (DNN) based procedure to predict the angle of arrival (AOA) and angle of departure (AOD) both in terms of azimuth and elevation, i.e., AAOA/AAOD and EAOA/EAOD. In order to evaluate the performance of the proposed procedure under practical assumptions, we employ a trajectory prediction method by considering dynamic window approach (DWA) to estimate the location information of the user equipment (UE), which is utilized as the input parameter of the trained DNN to generate the prediction of AAOA/AAOD and EAOA/EAOD. The robustness of the prediction procedure is analyzed in the presence of prediction errors, which proves that the proposed DNN is a promising tool to predict AOA and AOD in NLOS scenarios based on the estimated UE location. Simulation results shows that the prediction errors of the AOA and AOD can be maintained within an acceptable range of $\pm 2°$.

INDEX TERMS Deep learning, mmWave, NLOS, trajectory prediction, estimation.

I. INTRODUCTION

THE EXPLOSIVE demand in users' mobile data experience makes an increasing strain on the network's use of the available wireless spectrum. In order to solve this issue, one of the most important missions for the telecommunications industry is to explore higher frequency in wireless communication networks [1]. As such, in the fifth-generation of wireless communication networks (5G), millimeter wave (mmWave) frequencies, ranging from 30-300 GHz, are being explored to overcome the spectrum shortage. With its rich spectrum resources, mmWave can support high data rate transmissions, which makes mmWave one of the most promising technologies in future wireless networks [1]–[5]. However, mmWave also faces some challenges, such as high propagation loss, resulting in short propagation distances, and signal blockage caused not only by building materials and foliage, but also human body and high oxygen absorption [6].

To address the path loss issues of mmWave communications, one effective solutions is beamforming [7], which brings plenty of benefits, such as better coverage at a cell's edge, improved signal quality, tracking the user equipment (UE), and allowing cooperation among base stations (BSs). Although directional beamforming helps compensate for the significant path loss incurred by mmWave signals, it comes up with a complex beam alignment issue. More specifically, it is essential for a BS to know the angle of arrival (AOA) and the angle of departure (AOD) of its users in order to determine the beamforming direction.[1] A natural approach to perform beamforming training to improve the alignment accuracy is to exhaustively search for all possible pairs to identify the best beam alignment [8]. When there are only line-of-sight (LOS) channels in the mmWave communication system, the exhaustive search procedure has a calculation complexity of exponential growth [9]. With dense base station deployment, signals are able to be transmitted through LOS channel, however, due to the dynamics of the environment (e.g., blocking because of the UE mobility, and the high deployment cost of mmWave) the LOS channel might not be

1. Note that the state of the art algorithms typically use precoding vectors for beamforming, which is essentially a function of the AOA and DOA.

always available. In this case, the non-light-of-sight (NLOS) link should be considered to solve the coverage issues, which can be established when a reflective path exists between the transmitter and receiver [10], [11].

With NLOS propagation, multiple copies of the transmitted signals arrive at different times at the receiver, each with a different amplitude [12]. Due to the nature of narrow beams in mmWave communication, only limited number of angles can be covered by a beam. In this case, to identify the most suitable NLOS channel, the BS can search the obstacles surrounding the UE, such as buildings, and pick up the possible buildings as the reflector to form the NLOS channel. However, there could be many reflectors in the urban city scenario around UEs, leading to high complexity and latency, especially when UE has a mobility thus discontinuous angle change is expected due to the blockage. Moreover, these surfaces may have significantly different reflecting factors, which could affect the received signal power. To identify which surface is the best reflector, an efficient way is to find the AOA and AOD of the strongest received power beam of the NLOS path [13]. Therefore AOA and AOD for mmWave beam in NLOS scenario are the key parameters required for determining the suitable NLOS propagation path for a UE.

However, if current techniques, such as exhaustive beam search are applied, a significant overhead and a heavy computational burden can be imposed on the system. In order to solve this issue, Machine learning (ML) [14] is a potential method, which has received great attention due to its capability of finding valuable and hidden patterns from huge unknown datasets, such as in channel information [15]. On one hand, ML is extremely flexible and accurate in making predictions. On the other hand, massive data in the communication system is easy be to obtained. Thus, communication systems can benefit a lot with plenty of data [16]. Further, when compared to traditional methods, ML can learn complex relationships between raw input and output data through a training process [17]. Based on the intrinsic parameters of the collected data found by ML, predictions can be done with a trained model. This brings some advantages to ML over mathematical methods, such as, not relying on a specific mathematical models, resulting in flexible and adaptable algorithms, and being able to learn just from data.

It is quite challenging to identify the AOA and AOD of NLOS channels in wireless networks, mainly due to the user mobility, since the surrounding environment is constantly changing. Especially, it is more practical to assume that the UE location is unknown in such an estimation [18]. In this case, a UE trajectory prediction algorithm could be a utilized. By generating the channel information of the whole NLOS area and training the deep neural network (DNN) with part of the channel information, we can first predict the trajectory of the UE to obtain its location information from the trajectory prediction algorithm (TPA). With the estimated location information as an input, the trained neural network is utilized to predict the AOA and AOD of the potentially best NLOS beam for each position on the UE's predicted path.[2]

In this paper, we create a NLOS simulation model to generate the datasets, consisting of received power, location, and the number of clusters from raw data obtained by K-means, which is used to train a DNN without UE monility prediction. This trained DNN is then used to estimate the AOA and AOD in given positions. After the training, we form a new dataset, where the position of the UE is unknown to the trained DNN. In this case, the TPA is applied to predict the UE and generating the location information. Based on that, we test the DNN and estimate both the next position as well as AOA and AOD of NLOS channel. Lastly, a comparison in terms of predicting AOA/AOD between convolutional neural networks (CNN) and our networks is performed. The main contributions of this paper are summarized as follows.

1) A procedure for predicting the AOA/AOD of the potentially best NLOS beam based on a DNN for a 3D mmWave outdoor scenario is proposed. With the dataset including, received power, location, and the number of clusters from raw data obtained by K-means, the trained neural network can predict the AOA/AOD of NLOS beams in the azimuth and elevation.
2) In order to make the simulation scenario more practical, we assume that the location information is unknown to the trained DNN. In this case, a robot path plan is utilized to design the TPA for UE to generate the location information. With the new location information predicted by TPA as an input of the trained DNN, AOA and AOD are estimated. Results show that the trained neural network can predict the AOA/AOD with very low loss around 0.02%. Moreover, our DNN algorithm is compared with CNN in the case of training and predicting AOA and AOD with the dataset consisting of known location information to prove our model is more suitable for predicting and estimating AOA and AOD in NLOS channel.

The rest of this paper is organized as follows. Related work is discussed in Section II. The system model of our simulation, including simulation environment design, DNN structure, data collection, and trajectory prediction are stated in Section III. The procedure and basic principle of predicting the AOA/AOD of potentially best NLOS beam and UE possible trajectory is proposed in Section IV. In Section V, we discuss and analyze the results and we perform the robust check on our system. Conclusion and future works are summarized in Section VI.

II. RELATED WORK

The channel feasibility of mmWave NLOS outdoor mobile communication was demonstrated in [18] via an experimental campaign. They found that although some well-known

2. Note that when we input the predicted UE location information into the trained DNN, the data is completely unfamiliar for the DNN.

lossy objects such as the human body have poor penetration, they can be treated as good reflectors at mmWave frequency. In [15], the authors proposed an Artificial intelligence (AI) enabled procedure to predict channel statistical characteristics based on convolutional neural networks (CNN) to obtain the mapping relationship between the location information of transmitter and receiver antennas. In [17], a channel condition identification method using a recurrent neural network structure with a long short-term memory block was proposed. Specifically, the authors classified NLOS and LOS channels with ML. An efficient deep learning model to predict optimal mmWave beam and blockage status was presented in [19]. Their method can not only predict mmWave beams and blockages with success probabilities but also predict the optimal mmWave beams to approach the upper bounds while requiring no beam training overhead. The authors in [20] discussed and evaluated typical neural network architectures that are suitable to the beamformed fingerprint positioning problem in NLOS positions. Regarding trajectory prediction, an efficient vehicle trajectory prediction framework based on a recurrent neural network was proposed in [21]. In the framework, ML was employed to analyze the temporal behavior and predict the future coordinates of the surrounding vehicles. On the other hand, the dynamic window approach to reactive collision avoidance was proposed in [22]. The authors in [23] provided some use cases of beam management in a V2X scenario. Among them, the initial beam alignment, beam tracking, and beam recovery cases are also the considerable cases in the mmWave beam management in the urban scenario. A field experiments on the downlink throughput performance of beam tracking in small cell BS was presented in [24]. The authors showed that in NLOS scenario, although the signal quality reduces due to the reflection, it is still possible for the UE to connect to the access point through the reflected paths. A practical experiment was conducted in [25] to prove that a connection between BS and UE can be maintained in NLOS mobility scenario, however, the throughput is limited because of low effective scatterers. Further, authors in [26] employ the reinforcement learning method for the beam managementf in mmWave, which is aim to explore the channel information, such strongest received power, AOA/AOD, path loss and etc..

III. SYSTEM MODEL

In this section, we present the channel model based on our research, specifically the received power and AOA/AOD.

In the system model, we consider that there is a single BS and a single UE. We utilize the ray tracing software, Wireless Insite to build the simulation environment. Ray tracing is a classical deterministic method used or modeling radio propagation. By tracing paths in the simulation environment, the received power can be obtained as [27]

$$P_R = \sum_{i=1}^{N_P} P_i, \tag{1}$$

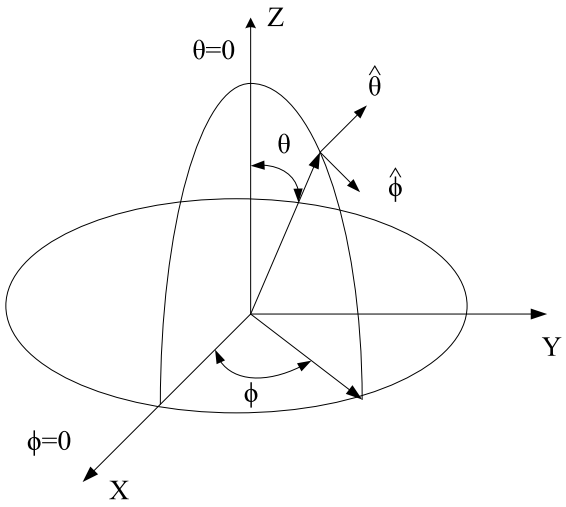

FIGURE 1. The Wireless InSite spherical coordinate system.

where N_P is the number of paths and P_i is the time averaged power in watts of the i^{th} path. P_i is given as

$$P_i = \frac{\lambda^2}{\pi \eta_0} \left| E_{(\theta,i)} g_\theta(\theta_i, \phi_i) + E_{(\phi,i)} g_\phi(\theta_i, \phi_i) \right|^2, \tag{2}$$

where λ is the wavelength, η_0 is the impedance of free space, $E_{(\theta,i)}$ and $E_{(\phi,i)}$ are θ and ϕ components of the electric field of the i^{th} path at the receiver point, respectively, and g_θ and g_ϕ are the direction of arrival of path i from the θ and ϕ directions, is given by

$$g_\theta(\theta_i, \phi_i) = \sqrt{\left(|G_\theta(\theta_i, \phi_i)| e^{j\phi_\theta} \right)}, \tag{3}$$

where G_θ is the θ component of the receiving antenna gain, and ψ_θ is the relative phase of the θ component of the far zone electric field.

The way to calculate AOA and AOD in azimuth and elevation angles are related to the antenna in the Wireless Insite (WI) software [28]. The location, orientation, and polarization of the antenna are set by the location of the associated transmitter or receiver and the rotation angles about the X, Y, and Z axis for each association of the antenna with a transmitter or receiver. The coordinate system used for singular rotation is shown in Fig. 1.

In this case, the angles θ_A and ϕ_A, with reference to the spherical coordinate system, give the direction from which the propagation path arrives at a receiver point. From Fig. 1, the AOA in azimuth and elevation angles can be obtained as

$$\hat{a} = \sin(\theta_A)\cos(\phi_A)\hat{x} + \sin(\theta_A)\cos(\phi_A)\hat{y} + \sin(\theta_A)\cos(\phi_A)\hat{z}. \tag{4}$$

Similarly, the AOD in azimuth and elevation angles can be obtained as

$$\hat{h} = \sin(\theta_H)\cos(\phi_H)\hat{x} + \sin(\theta_H)\cos(\phi_H)\hat{y} + \sin(\theta_H)\cos(\phi_H)\hat{z}. \tag{5}$$

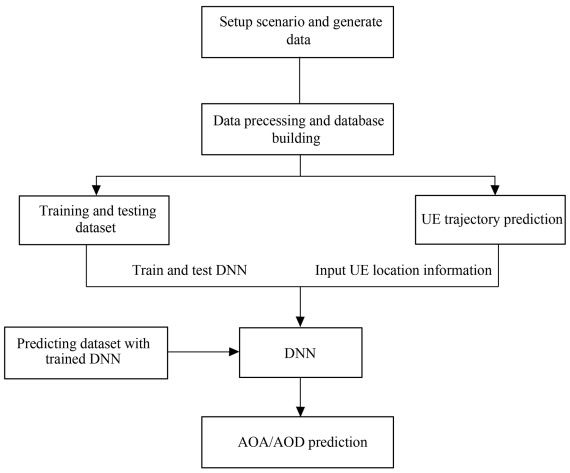

FIGURE 2. Flowchart showing the procedure for DNN enabled beam tracking in millimeter wave communications.

Regarding the UE position, the whole considered area consists of a rectangle, divided into N grids of one meter squared. We number the position coordinate from the first position on the lower left corner of the area to the last position on the top right corner. The UE can move to the nearest four grids in four different directions (up, down, left, and right) with the velocity of one meter per second. Further, it is also considered that the UE is able to avoid obstacles. In other words, if there is an obstacle in front of the UE, it has to find another way to go around the obstacles. More specifically, the UE and obstacles have their own radius. While UE is moving, for every step the algorithm calculates the distance between the UE and the nearby obstacle. If the distance is smaller than the UE's radius, the algorithm will find another direction for the UE's next move, else the UE will keep moving on the previous direction. The details are stated in Section IV-C.

IV. DEEP LEARNING BASED BEAM TRACKING APPROACH

In this section, we present the procedure for the ML based AOA/AOD prediction based on the analysis of UE trajectory in NLOS millimeter wave communications. The flow chart of the procedure is shown in Fig. 2.

With the simulation environment described in Section III, we obtain the raw network datasets [29], including the received signal power, AOA, AOD, and actual UE location information. Further, we process the raw data into the right data, which is suitable for the training of the neural network.

With the processed data, we train the DNN to predict the AOA/AOD in azimuth and elevation. The DNN is trained by 70% data with the received power, location information and the number of clusters from raw data obtained by K-means as the input. In the following, we present the main procedures involved in the DNN enabled beam tracking, namely data processing and database building, AOA/AOD prediction and the UE trajectory prediction.

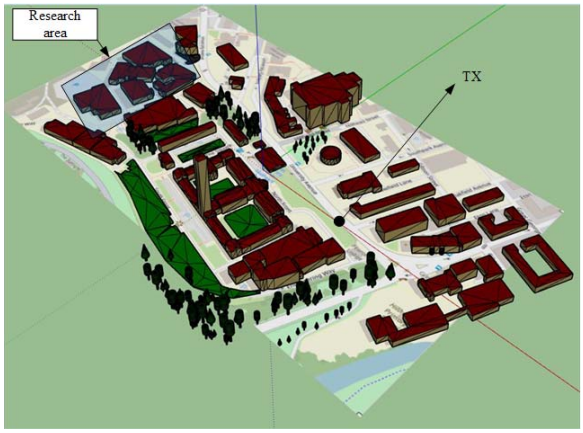

FIGURE 3. Simulation Environment (Based on The University of Glasgow campus, Gilmore Hill, UK).

When training the DNN, apart from AOA and AOD, other parameters such as received power, real UE location information, and a cluster by K-means are also considered as inputs of the DNN. With the trained DNN, we input only predicted UE locations into it, which is predicted by the UE trajectory prediction algorithm so that the DNN can predict the AOA and AOD with the predicted UE locations. To evaluate the performance of our AOA and AOD prediction, we calculate the error between the predicted AOA and AOD with the real AOA and AOD on different locations.

A. DATA PROCESSING AND DATABASE BUILDING

The simulation environment, which is based on the University of Glasgow Gilmorehill campus. The ray tracing software, Wireless InSite (WI), is used to build the simulation environment. Ray tracing is based on geometrical optic (GO) and the uniform theory of diffraction (UTD). The interactions between rays and objects can be classified as reflection, transmission, scattering, and diffraction. An area (shaded in blue in Fig. 3) of $X \times Y$ meters, was considered in WI, with N grid positions for the UE to move. In this simulation scenario, we have one receiver and one transmitter, with $X \times Y$ available positions. We do not consider scattering which is caused by surface roughness, due to the complexity of the simulation environment.

After collecting the raw network datasets from the simulated environment, we label received power, AOA in azimuth (AAOA), AOD in azimuth (AAOD), AOA in elevation (EAOA), AOD in elevation (EAOD), and user location as features. We divide the whole dataset into training and test datasets based on the ratio 7:3. After that, we apply K-means clustering to the raw data, which creates another feature that improves the DNN training accuracy. K-means clustering is a method that partitions n observations into k clusters in which each observation belongs to the cluster with the nearest mean [30]. The K-means algorithm classifies the raw data in different classes. Thus, we have metrics containing the different classes divided by the K-means method. In this case,

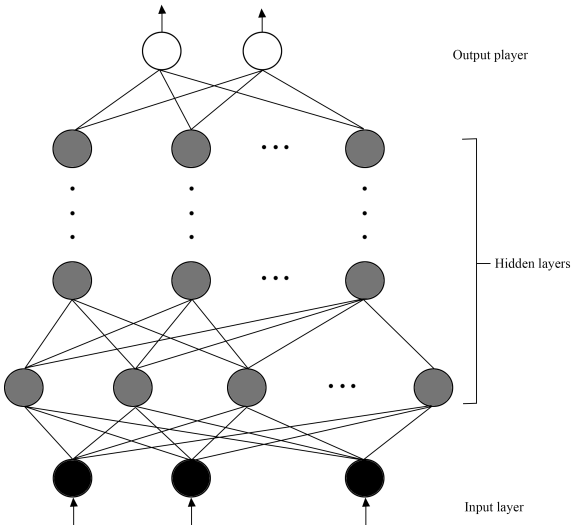

FIGURE 4. Basic DNN structure.

we have different features for DNN training: received power, AOA in azimuth (AAOA), AOD in azimuth (AAOD), AOA in elevation (EAOA), AOD in elevation (EAOD), and user location. However, due to the different units among these features, we first normalize the input data before we input the data into neural network. By normalization, we compute the deviation of the data from the mean and we divide it by the standard deviation. The transformed value of the input value x_{norm} after standardization can be expressed as

$$x_{norm} = \frac{(high - low) \times (x - \min X)}{\max X - \min X}, \tag{6}$$

where *high* and *low* are the range of data after scaling. $\max X$ and $\min X$ are the minimum and maximum value of the attribute X of input dataset [31].

However, we cannot use the transformed data to calculate the error between the real AOA/AOD and the predicted AOA/AOD. In this case, after AOA/AOD is predicted with the trained neural network, we apply the inverse-normalization to transform the data into its real form.

B. AOA/AOD PREDICTION BASED ON DNN

1) DNN DESIGN

Artificial neural network (ANN) is a computing system which is inspired by biological neural networks [32]. Generally, DNNs are deeper version of ANNs with more hidden layers to improve its representation or recognition ability [33]. The basic structure of a DNN is shown in Fig. 4.

The input layer is at the bottom. Each node on the input layer, shown in the figure refers to the number of inputs inserted in the DNN. The output layer is at the top, and the number of nodes stands for the number of outputs coming out from the DNN. In the middle of the DNN, there are some hidden layers, which have strong relevance with the design of DNN. Each neuron on the hidden layer in the network is actually a non-linear transform. For example, the relu

TABLE 1. Parameter of neural network.

Layers	Nodes	Activation
Input	1028	Relu
Dropout	N/A	N/A
Hidden Layer 1	512	Relu
Hidden Layer 2	256	Relu
Hidden Layer 3	128	Relu
Hidden Layer 4	64	Relu
Output	4	Linear

function is a non-linear transform, which can be defined as $f(x) = \max(0, x)$. Relu has some advantages, such as fast convergence, less required data, and sparse activation, which are very important for short response time systems like the wireless communications system [34]. Therefore, the output of the network z is a cascade of nonlinear transformations of the input data I, which can be expressed as

$$z = f(I) = f^{(L-1)}\left(f^{(L-2)}\left(\cdots f^{(1)}(I)\right)\right), \tag{7}$$

where L is the number of layers and α are the weights of neural network.

In the DNN, the weights for the neurons are required to be optimized while training. Usually, in DNN, the number of hidden layers, and the number of nodes on hidden layers are large and thus it causes the DNN to be more complex [35]. However, there is a trade-off between the number of hidden nodes and the accuracy. In our case, the basic DNN structure of predicting AAOA and AAOD is shown in Table 1, where we have considered four hidden layers. The input features in our DNN are received signal power, location information of UE, clusters by K-means and AOA/AOD in elevation when we predict AOA/AOD in azimuth. The number of inputs we insert in the input layer for training DNN is 3, while the number of input nodes for each hidden layer are 1028, 512, 256, and 64. The number of outputs coming out from output layer is 4. The desired output in this DNN is AAOA, AAOD, EAOA, and EAOD.

The performance of the DNN can be improved by using some hyper parameters to address challenges such as overfitting and learning rate selection. Overfitting results in the model learning the statistical noise in the training data, and this causes poor performance when the model is evaluated on new data. One approach to reduce overfitting is to fit all possible neural networks on the same dataset and average the predictions from each model [36]. However, this is not feasible in practice because of the low efficiency [36]. Dropout is a regularization method that approximates the training of a large number of neural network neurons with different architectures in parallel [36]. While training, we randomly dropout some number of layer outputs with dropout rate (one of the hyper-parameters) 0.4 for predicting AOA and AOD in azimuth and elevation. This makes the layer to be treated-like a layer with a different number of nodes and connectivity to the prior layer.

Secondly, we add an initializer for the DNN on the input layer to initialize its weight. The aim of the initializer is to

prevent layer activation outputs from exploding or vanishing during the course of a forward pass through DNN. If exploding or vanishing happens, loss gradients will either be too large or too small to flow backward beneficially, and this makes the neural network to converge slower. The initializer we use is Xavier [37], which could maintain the variance of activation and back-propagated gradients all the way up or down the layers of the network. Xavier initialization sets a layer's weights to values ranging from a random uniform distribution to

$$\beta_{layer} = \pm \frac{\sqrt{6}}{\sqrt{n_i + n_{i+1}}}, \tag{8}$$

where n_i is the number of incoming network connections to the layer, and n_{i+1} is the number of outgoing network connections from a given layer.

Thirdly, we also test the performance of DNN predicting AOA and AOD in azimuth and elevation with different learning rates. The learning rate is another hyper-parameter in neural network training, which controls how much change is made to the model in response to the estimated error each time the model weights are updated. It has a huge influence on the speed of the training process. Large learning rates may lead to a sub-optimal set of weight or an unstable training process. On the other hand, small learning rates may result in a long training process or the system could even get stuck [38]. To find a suitable learning rate in each stage of training, we apply the adaptive learning rate gradient descent to the DNN. Because each stage adapts the learning rate, often some configurations are required in each stage. The specific activation function in hidden layers is Relu. Further, the activation function of output layer is linear activation function, which is defined as $y = cx$. It thus creates an output signal proportional to the input.

We use Adam optimization algorithm, which has been used for the classical stochastic gradient descent procedure to update network weights based on training data [37]. The Adam optimization algorithm has a number of benefits, such as low computational complexity, having little memory requirements, and its high suitability to problems with very noisy/or sparse gradients [39].

2) AOA AND AOD PREDICTION

The procedure of AOA/AOD prediction is presented in Algorithm 1. In this scenario, the location of UE is known and we use the actual UE location as the input when we train the DNN to predict. Specifically, to predict the AOA and AOD, we input the features generated with the method in Section IV-A and standardize all the features in order to have them on the same scale. Then the DNN is configured via the method stated in Section IV-B (1) to improve the performance of our system.

After training the DNN, we input the same features from a test dataset into the trained neural networks to predict the AOA/AOD using the actual UE location as input. We calculate the absolute error between the predicted AOA/AOD and the real values to evaluate the prediction performance. Further, we generate some errors with truncated normal distribution which we add to the angle feature input in the DNN in order to evaluate the performance of our system in the presence of errors. The reason why we do so is that, in practice, there might be some errors when generating the data. If our system retains good performance, it means that our system is robust enough to measurement errors. The upper bound and lower bound of truncated normal distribution range from ± 10, ± 7, ± 5, and ± 2 (degree). According to the experience, the threshold for the mmWave beam signal is $\pm 7°$. We expect our system to retain a high AOA/AOD prediction accuracy for a degree of error below $\pm 7°$.

Algorithm 1: DNN Enabled AOA and AOD Prediction

Input: Received power, location information, and clusters by K-means in the training dataset

Output: Errors between real AOA/AOD and predicted AOA/AOD

initialization;

1. Normalize the input data;
2. Input the data into neural network;
3. Add dropout layer and initializers into neural network;
4. Train the neural network;
5. Input the location information in testing dataset into trained neural network;
6. Generate predicted AOA and AOD;
7. Calculate the absolute errors between real AOA/AOD and predicted AOA/AOD;

C. UE TRAJECTORY PREDICTION DESIGN

The dynamic window approach (DWA) proposed in [40] is used here for the reactive collision avoidance for the UE. DWA is executed with a fixed frequency, and only a set of velocities can be applied to the UE due to its acceleration and velocity limits. Among the set of velocities, a reward function is proposed to select the best velocities to follow [41]. The approach is directly from the motion dynamics of the UE. The motion can be obtained as follows

$$x(t_n) = x(t_0) + \int_{t_0}^{t_n} v(t) \cdot \cos\theta(t) dt, \tag{9}$$

$$y(t_n) = y(t_0) + \int_{t_0}^{t_n} v(t) \cdot \sin\theta(t) dt, \tag{10}$$

where $x(t)$ and $y(t)$ are the UE's coordinate at time t in the cartesian coordinate system, while the UE's orientation is dictated by $\theta(t)$ and t_0 is the initial time while t_n can be any time when the UE is moving.

The motion of the UE is constrained in a way that the translational velocity v always leads in the steering direction θ of the UE, which is called a non-holonomic constraint [42]. In the DWA, the search for commands controlling the UE is carried out directly in the space of velocities. The dynamics

of the UE are incorporated into the method by reducing the search space to those velocities that are reachable under the dynamic constraints. Due to these constraints, only velocities which are safe with respect to the obstacles are considered. Then by substituting the corresponding initial kinematic and dynamic configuration $v(t_0)$, $\theta(t_0)$, and $\omega(t_0)$ into (9) and (10), we obtain

$$x(t_n) = x(t_0) + \int_{t_0}^{t_n} \left(v(t_0) + \int_{t_0}^{t} \left(\dot{v}(\hat{t}) d\hat{t} \right) \right) \cdot \cos\left(\theta(t_0) + \int_{t_0}^{t} \left(\omega(t_0) + \int_{t_0}^{\hat{(t)}} \dot{\omega}(\tilde{t}) d\tilde{t} \right) d\tilde{t} \right) \mathrm{d}t. \quad (11)$$

Equation (11) is now in the form that the trajectory of the UE depends exclusively on its initial dynamic configuration at time t_0 and its accelerations. However, in our case, the angular velocity θ is discrete, and θ is in a set $\theta \in \{\theta_1, \theta_2, \theta_3, \theta_4\}, \forall\ 0 \leq \theta \leq \pi$. The values are evenly spaced by a θ_{step}, which will create a different number of directions for a single UE. To take into account the limited accelerations exertable by the UE, the overall search space is reduced to the DWA. It contains only the velocities that can be reached within the next time interval. In this case, t is the time interval during which accelerations $\dot{v}$ and $\dot{\omega}$ will be applied, considering (v_a, ω_a) as the actual velocity of a given UE, the dynamic window V_d is defined as

$$V_d = (v, \omega) | v \in [v_a - \dot{v} \cdot t, v_a + \dot{v} \cdot t] \wedge \omega \in [\omega_a - \dot{\omega} \cdot t, \omega_a + \dot{\omega} \cdot t], \quad (12)$$

The dynamic window is centered around the actual velocity and the extensions of it depend on the accelerations that can be exerted. The alignment of the UE with the target direction is measured by target heading (v, ω). It is given by $180 - \theta$, where θ is the angle of the target relative to the UE's heading direction, as shown in Fig. 5.

In order to make the UE trajectory prediction scenario closer to the simulation environment, we zoom in the simulation area shown in Fig. 3 and create a new scenario for trajectory prediction, as shown in Fig. 6.

We assume that a UE (red cross), with the limited radius, randomly appears at the location indicated by a yellow cross within the area of interest and that the UE has a destination point indicated with a blue cross. For every step, the UE detects the obstacles (black points) in eight different directions and it calculates the distance between itself and the nearest obstacle or destination point. The UE finally stops at the destination point when the distance is smaller than its radius. Before the UE stops, the DWA will predict the possible directions on every step of the UE, which is shown as a green line. When the UE arrives at its destination, its path in the areas of interest is shown as a red line. The coordinate on the predicted path will be recorded as the location information. The whole procedure is based on collision avoidance. We set the destination of the UE in our scenario, which the UE tries to reach while avoiding the blockages on its path, such as buildings and trees.

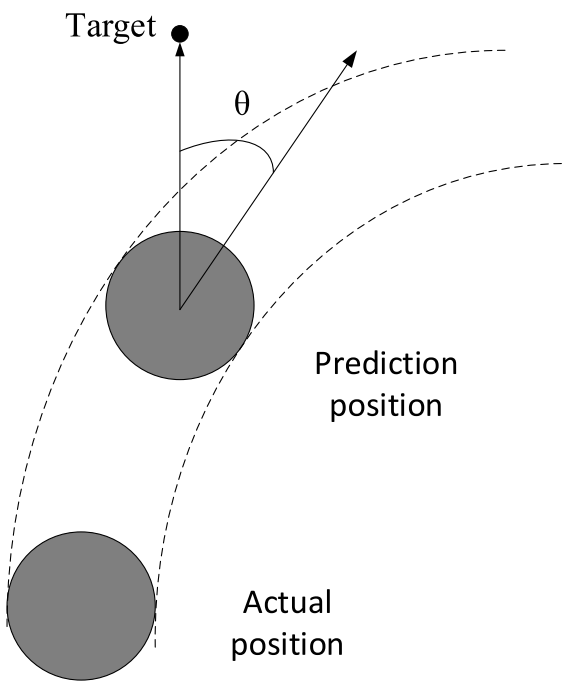

FIGURE 5. Target direction within DWA.

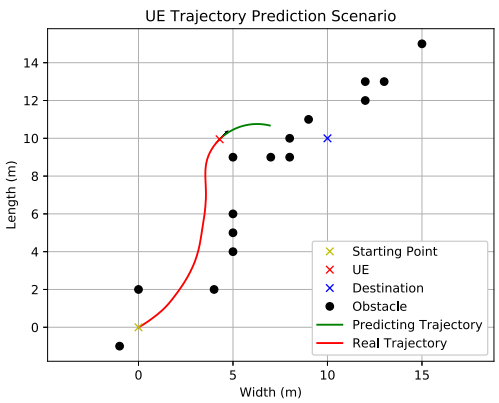

FIGURE 6. UE trajectory prediction.

In this procedure, we generate a total of 30 location information with a random starting point of the UE and we inverse the value of location information in the coordinate in the scale of the campus simulation environment. The AOA and AOD prediction with UE trajectory prediction is our second simulation scenario. Based on trained DNN, we replace the actual UE location information generated from the campus simulation environment with the predicted UE location information and we input it into the trained DNN in order to predict the AOA/AOD. After that, we do another simulation to evaluate the performance of our method when the angle information are with some errors. Similar to the simulation in Section IV-B, we generate some errors with truncated normal distribution, in which the upper limit and lower limit range

TABLE 2. Parameters in simulation environment.

Transmit power	43 dBm
Carrier Frequency	30 GHz
Noise	-88 dBm
Effective Bandwidth	200 MHz
TX Height	40 m
Area Length (X)	223 m
Area Width (Y)	328 m
Number of Grid Positions (N)	73696

from ±10, ±5, and ±2 degree. We add the errors on the predicted location information, which we input into the same trained DNN to evaluate the performance of our method. Note that ±10 meters are large errors for the prediction. On the other hand, ±5, and ±2 are allowable errors for trajectory prediction. Although there are such errors, our system still can make most of UE position access to the BS. This simulation shows the robustness of our system to prediction errors. With this simulation, the error tolerance of our system is proven. Detailed results are presented in the next section.

V. RESULTS AND DISCUSSION

We conduct experiments to evaluate the performance of the AOA/AOD estimation with deep learning. We first predict the AOA and AOD with the trained DNN using some of given UE locations. After that, we assume the UE locations are unknown, with the AOA and AOD angles in azimuth and elevation being estimated based on the UE trajectory prediction proposed in Section IV-C. We evaluate the performance of the predication algorithm in the presence of errors showing its robustness. Secondly, we compare the performance of our proposed method with another typical ML method – CNN, in terms of accuracy in the prediction of EAOA and EAOD. The parameters of the simulation settings are shown in Table 2.

A. AOA AND AOD PREDICTION WITH PERFECT TESTING DATA

We start with the AOA and AOD prediction by training the DNN. In this work, the features used to train the DNN consists of received power, location information, and clusters by K-means. The training performance is shown in Fig. 7, where the loss function is given by the mean square error (MSE), which is defined as:

$$MSE = \frac{1}{n}\sum_{i=1}^{n} e_i^2, \tag{13}$$

where e_i is the training error by the i-th sample and n is the total number of samples.

As it can be seen, the loss curve converges after 300 epochs and the testing loss curve fluctuates slightly. The reason is that when the UE position changes, there is few changes on AOA and AOD. However, both training loss and testing loss maintain a very low level (0.02), which is acceptable for DNN training.

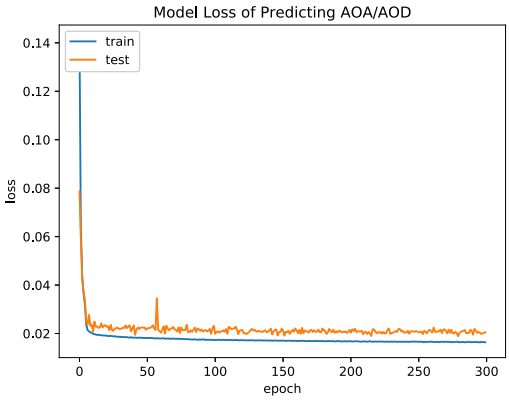

FIGURE 7. Performance of training DNN to predict AOA/AOD.

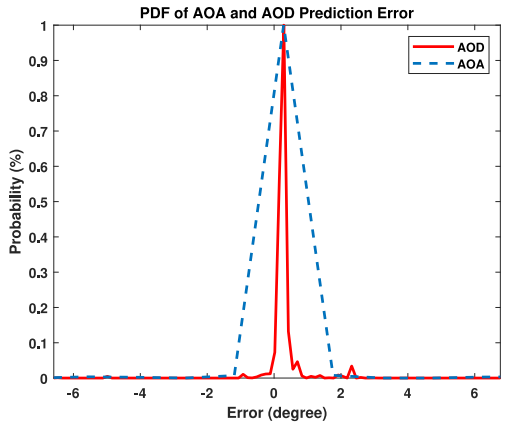

FIGURE 8. PDF of AOA/AOD predicted error.

Based on the trained DNN, we input features from the test dataset to predict AOA and AOD, which consists of complete new unseen samples for the trained DNN. We calculate the absolute error between the predicted and real values and show the results of the probability density functions (PDF) of prediction errors. From Fig. 8, the AOA prediction absolute error (blue line) keeps in around ±2°. We define if the error is over 7°, it will be out of connection from BS. Then we calculate the number of positions in testing dataset, which are out of connection from BS. There are 40 out of 7034 positions out of connection with BS (the percentage is about (0.5%)). Further, for AOD prediction absolute error (red line), we can see that the error percentge is around 7/7034 (0.1%). However, despite these minor variations, the proposed DNN method is able to achieve accurate predictions for both AOA and AOD with an error below 7°.

B. PREDICTION PERFORMANCE WITH IMPERFECT TESTING DATA

Next, we explore the performance of the proposed DNN with imperfect testing dataset, which is more related to the practical scenario. We do this by adding errors into features, specifically AOA and AOD of the test dataset for AOA and AOD prediction. The errors follow a truncated normal distribution and the upper and lower bounds are ±10°, ±7°, and

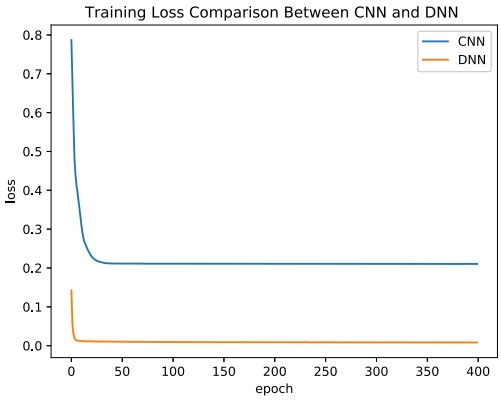

FIGURE 9. Training loss comparison between CNN and DNN.

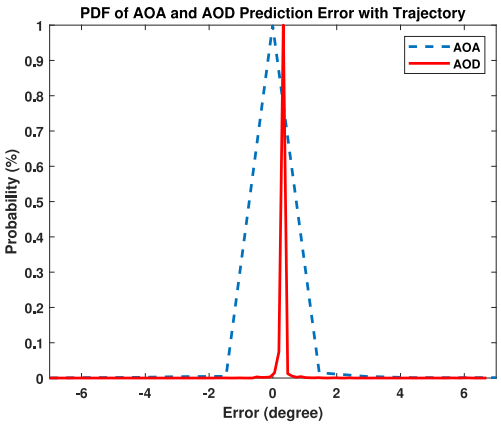

FIGURE 10. PDF of AOA/AOD predicted error with trajectory prediction.

$\pm 2°$. In our experience, if the AOA and AOD prediction errors are over $\pm 10°$, the UE will be out of connection with the BS. When the bound is between $\pm 10°$ and $\pm 7°$, the UE has connection with BS but poor signal quality. The signal quality will be better with the error reducing. When the bound is between $\pm 7°$ and $\pm 2°$, the UE will have the prosperity communication experience with the BS. The performance of the proposed algorithm under imperfect testing dataset is shown in Table 3, in addition to the case with no errors. From Table 3, it can be seen that our system can still maintain a very low prediction error when the added errors are smaller than the threshold. This clearly shows the robustness of our system and the advantage of utilizing machine learning, more specifically DNN, than other methods. We add some errors into the dataset to make it more particular. The results show that the predication algorithm can maintain the accuracy when the added errors are smaller than $\pm 7°$.

Further, in order to make a comparison with other method, we also evaluate the performance of a CNN-based prediction of AOA and AOD. The results are shown in Fig. 9. As it can be seen, the loss generated by the CNN is much higher than that of the DNN and even by increasing the number of epochs, it can be seen that it does not improve. The reason

TABLE 3. Prediction performance in the present of errors.

Scenarios	AOD	AOD
No Error	7 (0.1%)	40 (0.5%)
$2°$	10 (0.14%)	62 (0.8%)
$7°$	35 (0.5%)	81 (1.15%)
$10°$	3353 (47%)	3550 (50%)

for this is that architecture of the CNN is not good for this problem and CNN is more suitable for receiving and processing pixel data. However, our dataset is consisted of numeral numbers.

C. AOA/AOD PREDICTION WITH UE TRAJECTORY PREDICTION

In this simulation, we generate UE locations predicted by DWA for 30 times with a random starting point, as stated in Section IV-C. We input the location information as the only feature into the trained DNN for AOA and AOD prediction. From Fig. 10, AOA and AOD prediction error with trajectory prediction are located around $\pm 2°$, which maintain closed level with AOA and AOD predicted error. As mentioned in Section IV-C, the dynamic window approach is a reactive collision avoidance algorithm. The BS could locate the UE position and be aware of the surrounding environment, such as buildings, streets, and road. In this case, based on collision avoidance principle of the UE, the dynamic window approach can predict the UE's route from its starting point to its destination. Therefore, the BS generates the location information of the predicted UE route. And based on the location information as the input of the DNN, the trained DNN can predict the AOA/AOD of the UE on each position of its route. From this experiment, it shows that our system has the ability to predict the UEs' AOA and AOD with totally unknown locations. The reason why the performance results of AOA/AOD prediction with UE trajectory prediction are better than the performance of only DNN based method shown in Fig. 8 is that when we input only location information generated by DWA, the trained DNN can be more easily focused. The reason behind is that when training the DNN, the weight of location information account for the majority. Thus, the accuracy of the prediction results rises. On the contrary, when we predict AOA and AOD via DNN without DWA (the performance is shown in Fig. 8), in addition to the location information, the inputs in the neural network also include received power and the number of clusters from raw data obtained by K-means. In this case, other factors may affect the result more even through the location information is accurate. Therefore, the prediction results of Fig. 10 is slightly better than that of Fig. 8.

D. COMPUTATION COMPLEXITY

The comparison of computation complexity between traditional method such as exhaustive search and our method is made in this section. The exhaustive search browses all possible AOA/AOD and chooses the best result. However,

when we compared the predicted outcome of AOA/AOD with the particular value to generate the prediction error, the particular value is already the best received power, which is as same as the exhaustive search result for each position in the simulation area. We consider the online deployment part of our method and searching part of the exhaustive search method. More specifically, only the prediction procedure for each position of our method is under consideration rather that training part and for exhaustive search the channel estimation procedure is ignored. The equation we adapted to calculate the computation complexity of DNN is:

$$F = \sum_{i=2}^{n} \eta_i \times \eta_{i-1} + \sum_{i=1}^{n} \eta_i, \tag{14}$$

where η is the number of nodes in each layers and i is the layer. In this case, according to Table 1 (it can be found in the Appendix of this letter), we have one input layer with 1028 nodes, four hidden layers with 512, 256, 128, 128, and 64 nodes, and one output layer with 4 nodes. We assume that the number of additions and multiplications in the DNN have the same computation burden in our case. Therefore, the computation complexity of our method is the computation between each layers and the computation of activation function (Relu in our method) in each node, which is 6.99×10^5. For the exhaustive search, for each position, we have to consider both azimuth and elevation angle. When we calculate the prediction error, the precision is one degree. Therefore, we have 360 different angles to be considered for both azimuth and elevation. In this case, based on the simplest Bubble Sort computation complexity calculation, the computation complexity for exhaustive search is 1.67×10^9, which is around 42,000 times larger than our method.

VI. CONCLUSION

A deep learning enabled method to prediction the AOA and AOD in NLOS channel for mmWave communication is proposed in this paper. Firstly, we build the simulation model with NLOS scenario and channel model of AOA/AOD to generate the dataset for DNN training. We train the neural network with some channel features, such as received power, location. Results indicate that the absolute error, calculated between the real and the predicted are quite low, validating the effectiveness of the proposed solution. Further, we add some error with truncated normal distribution in the beam angle to evaluate the robustness of our system. When the error is below a given threshold of 7°, our system still has good performance. Finally, we predict the UE trajectory with DWA and generate location input. Further, input it into the trained DNN to evaluate the performance of trajectory prediction. The error in this case is close to the original location information from data generation.

REFERENCES

[1] M. Xiao *et al.*, "Millimeter wave communications for future mobile networks," *IEEE J. Sel. Areas Commun.*, vol. 35, no. 9, pp. 1909–1935, Sep. 2017.

[2] T. S. Rappaport *et al.*, "Millimeter wave mobile communications for 5G cellular: It will work!" *IEEE Access*, vol. 1, pp. 335–349, 2013.

[3] K. Yu and Y. J. Guo, "Statistical NLOS identification based on AOA, TOA, and signal strength," *IEEE Trans. Veh. Technol.*, vol. 58, no. 1, pp. 274–286, Jan. 2009.

[4] S. K. Sharma, T. E. Bogale, L. B. Le, S. Chatzinotas, X. Wang, and B. Ottersten, "Dynamic spectrum sharing in 5G wireless networks with full-duplex technology: Recent advances and research challenges," *IEEE Commun. Surveys Tuts.*, vol. 20, no. 1, pp. 674–707, 1st Quart., 2018.

[5] X. Xue, Y. Wang, X. Wang, and T. E. Bogale, "Joint source and relay precoding in multiantenna millimeter-wave systems," *IEEE Trans. Veh. Technol.*, vol. 66, no. 6, pp. 4924–4937, Jun. 2017.

[6] W. Roh *et al.*, "Millimeter-wave beamforming as an enabling technology for 5G cellular communications: Theoretical feasibility and prototype results," *IEEE Commun. Mag.*, vol. 52, no. 2, pp. 106–113, Feb. 2014.

[7] M. M. Molu, P. Xiao, M. Khalily, K. Cumanan, L. Zhang, and R. Tafazolli, "Low-complexity and robust hybrid beamforming design for multi-antenna communication systems," *IEEE Trans. Wireless Commun.*, vol. 17, no. 3, pp. 1445–1459, Mar. 2018.

[8] X. Wu *et al.*, "60-GHz millimeter-wave channel measurements and modeling for indoor office environments," *IEEE Trans. Antennas Propag.*, vol. 65, no. 4, pp. 1912–1924, Apr. 2017.

[9] C. Liu, M. Li, S. V. Hanly, P. Whiting, and I. B. Collings, "Millimeter-wave small cells: Base station discovery, beam alignment, and system design challenges," *IEEE Wireless Commun.*, vol. 25, no. 4, pp. 40–46, Aug. 2018.

[10] T. Mantoro, M. A. Ayu, and M. R. Nugroho, "NLOS and LOS of the 28 GHz bands millimeter-wave in 5G cellular networks," in *Proc. Int. Conf. Comput. Eng. Design (ICCED)*, 2017, pp. 1–5.

[11] J. C. Aviles and A. Kouki, "Position-aided mm-Wave beam training under NLOS conditions," *IEEE Access*, vol. 4, pp. 8703–8714, 2016.

[12] O. Abari, H. Hassanieh, M. Rodriguez, and D. Katabi, "Millimeter wave communications: From point-to-point links to agile network connections," in *Proc. 15th ACM Workshop Hot Topics Netw.*, 2016, pp. 169–175.

[13] Q. C. Li, G. Wu, and T. S. Rappaport, "Channel model for millimeter-wave communications based on geometry statistics," in *Proc. IEEE Globecom Workshops (GC Wkshps)*, 2014, pp. 427–432.

[14] P. Ferrand, M. Amara, S. Valentin, and M. Guillaud, "Trends and challenges in wireless channel modeling for evolving radio access," *IEEE Commun. Mag.*, vol. 54, no. 7, pp. 93–99, Jul. 2016.

[15] L. Bai *et al.*, "Predicting wireless mmWave massive MIMO channel characteristics using machine learning algorithms," *Wireless Commun. Mobile Comput.*, vol. 2018, Aug. 2018, Art. no. 9783863.

[16] M. M. Molu, P. Xiao, M. Khalily, K. Cumanan, L. Zhang, and R. Tafazolli, "Low-complexity and robust hybrid beamforming design for multi-antenna communication systems," *IEEE Trans. Wireless Commun.*, vol. 17, no. 3, pp. 1445–1459, Mar. 2018.

[17] J.-S. Choi, W.-H. Lee, J.-H. Lee, J.-H. Lee, and S.-C. Kim, "Deep learning based NLOS identification with commodity WLAN devices," *IEEE Trans. Veh. Technol.*, vol. 67, no. 4, pp. 3295–3303, Apr. 2018.

[18] S. Rajagopal, S. Abu-Surra, and M. Malmirchegini, "Channel feasibility for outdoor non-line-of-sight mmWave mobile communication," in *Proc. IEEE Veh. Technol. Conf. (VTC Fall)*, 2012, pp. 1–6.

[19] M. Alrabeiah and A. Alkhateeb, "Deep learning for mmWave beam and blockage prediction using sub-6GHz channels," 2019. [Online]. Available: arXiv:1910.02900.

[20] J. Gante, G. Falcão, and L. Sousa, "Deep learning architectures for accurate millimeter wave positioning in 5G," *Neural Process. Lett.*, vol. 51, no. 2, pp. 487–514, 2020.

[21] B. Kim, C. M. Kang, J. Kim, S. H. Lee, C. C. Chung, and J. W. Choi, "Probabilistic vehicle trajectory prediction over occupancy grid map via recurrent neural network," in *Proc. IEEE 20th Int. Conf. Intell. Transp. Syst. (ITSC)*, 2017, pp. 399–404.

[22] D. Fox, W. Burgard, and S. Thrun, "The dynamic window approach to collision avoidance," *IEEE Robot. Autom. Mag.*, vol. 4, no. 1, pp. 23–33, Mar. 1997.

[23] T. Shimizu, V. Va, G. Bansal, and R. W. Heath, "Millimeter wave V2X communications: Use cases and design considerations of beam management," in *Proc. Asia-Pac. Microw. Conf. (APMC)*, 2018, pp. 183–185.

[24] Y. Inoue, Y. Kishiyama, S. Suyama, J. Kepler, M. Cudak, and Y. Okumura, "Field experiments on 5G mmW radio access with beam tracking in small cell environments," in *Proc. IEEE Globecom Workshops (GC Wkshps)*, 2015, pp. 1–6.
[25] T. Kadur, H.-L. Chiang, and G. Fettweis, "Experimental validation of robust beam tracking in a NLoS indoor environment," in *Proc. 25th Int. Conf. Telecommun. (ICT)*, 2018, pp. 644–648.
[26] R. Wang *et al.*, "Reinforcement learning method for beam management in millimeter-wave networks," in *Proc. U.K./China Emerg. Technol. (UCET)*, 2019, pp. 1–4.
[27] *Remcom*. Accessed: Apr. 4, 2021. [Online]. Available: https://www.remcom.com/
[28] P. Mededović, M. Veletić, and Ž. Blagojević, "Wireless insite software verification via analysis and comparison of simulation and measurement results," in *Proc. 35th Int. Conv. MIPRO*, 2012, pp. 776–781.
[29] R. Wang, "Simulation dataset," *Google Drive*, Apr. 2021. Accessed: Jul. 12, 2021. [Online]. Available: https://drive.google.com/file/d/160G8q2VhSHIEakl-kHV9MynFxbKlaNfF/view?usp=sharing
[30] N. Srivastava, G. Hinton, A. Krizhevsky, I. Sutskever, and R. Salakhutdinov, "Dropout: A simple way to prevent neural networks from overfitting," *J. Mach. Learn. Res.*, vol. 15, no. 1, pp. 1929–1958, 2014.
[31] S. Bhanja and A. Das, "Impact of data normalization on deep neural network for time series forecasting," 2018. [Online]. Available: arXiv:1812.05519.
[32] Y.-Y. Chen, Y.-H. Lin, C.-C. Kung, M.-H. Chung, and I.-H. Yen, "Design and implementation of cloud analytics-assisted smart power meters considering advanced artificial intelligence as edge analytics in demand-side management for smart homes," *Sensors*, vol. 19, no. 9, p. 2047, 2019.
[33] J. Schmidhuber, "Deep learning in neural networks: An overview," *Neural Netw.*, vol. 61, pp. 85–117, Jan. 2015.
[34] Y. Li and Y. Yuan, "Convergence analysis of two-layer neural networks with ReLu activation," in *Proc. Adv. Neural Inf. Process. Syst.*, 2017, pp. 597–607.
[35] H. Ye, L. Liang, G. Y. Li, J. Kim, L. Lu, and M. Wu, "Machine learning for vehicular networks," 2017. [Online]. Available: arXiv:1712.07143.
[36] I. V. Tetko, D. J. Livingstone, and A. I. Luik, "Neural network studies. 1. Comparison of overfitting and overtraining," *J. Chem. Inf. Comput. Sci.*, vol. 35, no. 5, pp. 826–833, 1995.
[37] D. P. Kingma and J. Ba, "Adam: A method for stochastic optimization," 2014. [Online]. Available: arXiv:1412.6980.
[38] X.-H. Yu and G.-A. Chen, "Efficient backpropagation learning using optimal learning rate and momentum," *Neural Netw.*, vol. 10, no. 3, pp. 517–527, 1997.
[39] A. Paszke, A. Chaurasia, S. Kim, and E. Culurciello, "Enet: A deep neural network architecture for real-time semantic segmentation," 2016. [Online]. Available: arXiv:1606.02147.
[40] D. Fox, W. Burgard, and S. Thrun, "Controlling synchro-drive robots with the dynamic window approach to collision avoidance," in *Proc. IEEE/RSJ Int. Conf. Intell. Robots Syst.*, vol. 3, 1996, pp. 1280–1287.
[41] J.-P. Laumond, *Robot Motion Planning and Control*, vol. 229. Heidelberg, Germany: Springer, 1998,
[42] E. J. Molinos, Á. Llamazares, and M. Ocaña, "Dynamic window based approaches for avoiding obstacles in moving," *Robot. Auton. Syst.*, vol. 118, pp. 112–130, Aug. 2019.

RUIYU WANG received the B.Eng. degree in electrical and electronic engineering from the China University of Petroleum, China, in 2015, the M.Sc. degree in electrical and electronic engineering from the University of Sheffield, Sheffield, U.K., in 2017. He is currently pursuing the Ph.D. degree with the University of Glasgow, Glasgow, U.K. His research interests contain mmWave, beamforming, handover in small cell base station, and the application of machine learning in communication networks.

PAULO VALENTE KLAINE (Member, IEEE) received the B.Eng. degree in electrical and electronic engineering from the Federal University of Technology–Paraná, Brazil, in 2014, the M.Sc. degree in mobile communications systems from the University of Surrey, Guildford, U.K., in 2015, and the Ph.D. degree in electrical and electronics engineering from the University of Glasgow, U.K., in 2019, where he is currently a Research Associate. He has three filed patents and authored/coauthored over 15 publications. His research interests include self organizing networks, V2X communications, wireless blockchain, and machine learning in wireless networks.

OLUWAKAYODE ONIRETI (Senior Member, IEEE) received the B.Eng. degree (Hons.) in electrical engineering from the University of Ilorin, Ilorin, Nigeria, in 2005, and the M.Sc. degree (Hons.) in mobile and satellite communications, and the Ph.D. degree in electronics engineering from the University of Surrey, Guildford, U.K., in 2009 and 2012, respectively. He is currently a Lecturer with the University of Glasgow, U.K. He has been actively involved in projects such as ROCKET, EARTH, Greencom, QSON, DARE and, Energy proportional EnodeB for LTE-Advanced and Beyond. His main research interests include self-organizing cellular networks, millimeter wave communications, energy efficiency, wireless blockchain networks, and cooperative communications.

YAO SUN (Senior Member, IEEE) received the B.S. degree in mathematical science and the Ph.D. degree in communication and information system from the University of Electronic Science and Technology of China (UESTC), Chengdu, China, in 2014 and 2019, respectively. He was a Research Fellow with UESTC. He is currently a Lecturer with James Watt School of Engineering, University of Glasgow, Glasgow, U.K. He has extensive research experience in wireless communication area. He has published more than 30 peer-review papers, two book chapters, and three patents. His research interests include intelligent wireless networking, network slicing, blockchain system, Internet of Things, and resource management in mobile networks. He has won the IEEE Communication Society of TAOS Best Paper Award in 2019 ICC. He has been the guest editor for special issues of several international journals. He has been served as a TPC Member for number of international conferences, including GLOBECOM 2020, WCNC 2019, and ICCT 2019.

MUHAMMAD ALI IMRAN (Senior Member, IEEE) is a Professor of Wireless Communication Systems. He heads the Communications, Sensing and Imaging CSI Research Group, University of Glasgow and is the Dean of the University of Glasgow and UESTC. He is an Affiliate Professor with the University of Oklahoma, USA, and a Visiting Professor with the 5G Innovation Centre, University of Surrey, U.K. He has over 20 years of combined academic and industry experience with several leading roles in multi-million pounds funded projects. He has filed 15 patents; has authored/coauthored over 400 journal and conference publications; was an editor of five books and author of more than 20 book chapters; has successfully supervised over 40 postgraduate students at doctoral level. He has been a consultant to international projects and local companies in the area of self-organized networks. He has been interviewed by BBC, Scottish television, and many radio channels on the topic of 5G technology. His research interests in self organized networks, wireless networked control systems, and the wireless sensor systems. He is a Fellow of IET and a Senior Fellow of HEA.

LEI ZHANG (Senior Member, IEEE) received the Ph.D. degree from the University of Sheffield, U.K. He is a Senior Lecturer with the University of Glasgow, U.K. He has 19 U.S./U.K./EU/China granted/filed patents on wireless communications and published two books and over 100 peer-reviewed papers. His research interests include wireless communication systems and networks, blockchain technology, radio access network slicing (RAN slicing), Internet of Things, multiantenna signal processing, and MIMO systems. He received IEEE Communication Society TAOS Best Paper Award 2019. He is a Technical Committee Chair of 5th U.K.–China Emerging Technologies (UCET) 2020. He was the Publication and Registration Chair of IEEE Sensor Array and Multichannel 2018, a Publicity Chair of 4th UCET 2019, a Co-chair of Cyber-C Blockchain Workshop 2019. He is an Associate Editor of IEEE INTERNET OF THINGS JOURNAL, IEEE WIRELESS COMMUNICATIONS LETTERS, and *Digital Communications and Networks*.